INTERNATIONAL STANDARD

ISO 16808

Second edition
2022-05

Metallic materials — Sheet and strip — Determination of biaxial stress-strain curve by means of bulge test with optical measuring systems

Matériaux métalliques — Tôles et bandes — Détermination de la courbe contrainte-déformation biaxiale au moyen de l'essai de gonflement hydraulique avec systèmes de mesure optiques

Reference number
ISO 16808:2022(E)

ISO copyright office
CP 401 • Ch. de Blandonnet 8
CH-1214 Vernier, Geneva
Phone: +41 22 749 01 11
Email: copyright@iso.org
Website: www.iso.org

Published in Switzerland

Contents

Page

Foreword

ISO (the International Organization for Standardization) is a worldwide federation of national standards bodies (ISO member bodies). The work of preparing International Standards is normally carried out through ISO technical committees. Each member body interested in a subject for which a technical committee has been established has the right to be represented on that committee. International organizations, governmental and non-governmental, in liaison with ISO, also take part in the work. ISO collaborates closely with the International Electrotechnical Commission (IEC) on all matters of electrotechnical standardization.

The procedures used to develop this document and those intended for its further maintenance are described in the ISO/IEC Directives, Part 1. In particular, the different approval criteria needed for the different types of ISO documents should be noted. This document was drafted in accordance with the editorial rules of the ISO/IEC Directives, Part 2 (see www.iso.org/directives).

Attention is drawn to the possibility that some of the elements of this document may be the subject of patent rights. ISO shall not be held responsible for identifying any or all such patent rights. Details of any patent rights identified during the development of the document will be in the Introduction and/or on the ISO list of patent declarations received (see www.iso.org/patents).

Any trade name used in this document is information given for the convenience of users and does not constitute an endorsement.

For an explanation of the voluntary nature of standards, the meaning of ISO specific terms and expressions related to conformity assessment, as well as information about ISO's adherence to the World Trade Organization (WTO) principles in the Technical Barriers to Trade (TBT), see www.iso.org/iso/foreword.html.

This document was prepared by Technical Committee ISO/TC 164, *Mechanical testing of metals*, Subcommittee SC 2, *Ductility testing*, in collaboration with the European Committee for Standardization (CEN) Technical Committee CEN/TC 459/SC 1, *Test methods for steel (other than chemical analysis)*, in accordance with the Agreement on technical cooperation between ISO and CEN (Vienna Agreement).

This second edition cancels and replaces the first edition (ISO 16808:2014), of which it constitutes a minor revision. The changes are as follows:

— the designation of r_{1_100} in Table 1 has been modified;

— the title of Figure A.4 has been modified;

— Formula (B.2) has been modified;

— Annex A has been deleted and other annexes have been renumbered accordingly;

— the status of Annex A (formerly Annex B) has been changed to informative;

— minor editorial changes have been made to align with ISO/IEC Directives Part 2, 2021.

Any feedback or questions on this document should be directed to the user's national standards body. A complete listing of these bodies can be found at www.iso.org/members.html.

Metallic materials — Sheet and strip — Determination of biaxial stress-strain curve by means of bulge test with optical measuring systems

1 Scope

This document specifies a method for determination of the biaxial stress-strain curve of metallic sheets having a thickness below 3 mm in pure stretch forming without significant friction influence. In comparison with tensile test results, higher strain values can be achieved.

NOTE In this document, the term "biaxial stress-strain curve" is used for simplification. In principle, in the test the "biaxial true stress-true strain curve" is determined.

2 Normative references

There are no normative references in this document.

3 Terms and definitions

No terms and definitions are listed in this document.

ISO and IEC maintain terminology databases for use in standardization at the following addresses:

— ISO Online browsing platform: available at https://www.iso.org/obp

— IEC Electropedia: available at http://www.electropedia.org/

4 Symbols and abbreviated terms

The symbols and designations used are given in Table 1.

Table 1

Symbol	Designation	Unit
d_{die}	Diameter of the die (inner)	mm
d_{BH}	Diameter of the blank holder (inner)	mm
R_1	Radius of the die (inner)	mm
h	Height of the drawn blank (outer surface)	mm
t_0	Initial thickness of the sheet (blank)	mm
t	Actual thickness of the sheet	mm
p	Pressure in the chamber	MPa
rms	Standard deviation (root mean square)	-
ρ	Radius of curvature	mm
r_1	Surface radius for determining curvature	mm
r_2	Surface radius for determining strain	mm
r_{1_100}	Surface radius to determine curvature with a diameter of 100 mm	mm
a_i, b_i	Coefficients for response surface	-

Table 1 *(continued)*

Symbol	Designation	Unit
σ_B	Biaxial stress	MPa
e	Engineering strain	-
ε_1	Major true strain	-
ε_2	Minor true strain	-
ε_3	True thickness strain	-
ε_E	Equivalent true strain	-
l_s	Coordinate and length of a section	mm
dz	Displacement in the z-direction	mm
dz_{mv}	Displacement after movement correction	mm

5 Principle

A circular blank is completely clamped at the edge in a tool between die and blank holder. A bulge is formed by pressing a fluid against the blank until final fracture occurs (Figure 1). During the test, the pressure of the fluid is measured and the evolution of the deformation of the blank is recorded by an optical measuring system[1],[2],[3]. Based on the recorded deformation of the blank, the following quantities near the centre of the blank are determined: the local curvature, the true strains at the surface, and, by assuming incompressible deformation of the material, the actual thickness of the blank. Furthermore, assuming the stress state of a thin-walled spherical pressure vessel at the centre of the blank, the true stress is calculated from the fluid pressure, the thickness and the curvature radius.

NOTE In addition to the bulge test procedures with optical measurement systems introduced in Reference [1] and described in the following, there are also laser systems[4],[5],[6] or tactile systems[7],[8],[9] valid for bulge test investigation, which are not covered in this document.

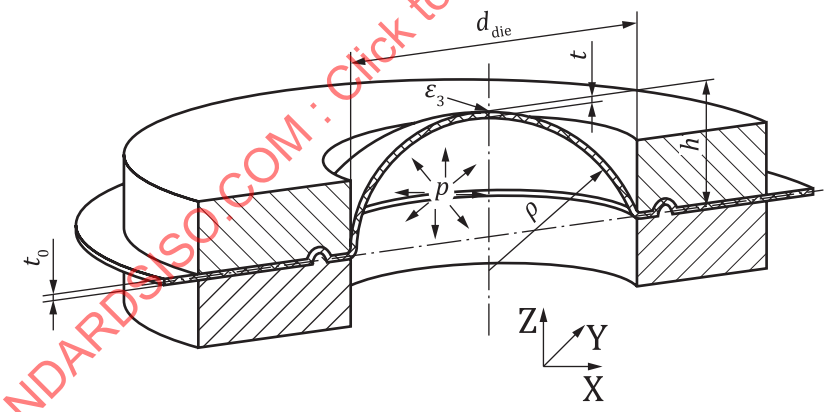

Key

h	height of the drawn blank (outer surface)	ρ	radius of curvature
p	pressure in the chamber	t_0	initial thickness of the sheet (blank)
ε_3	true thickness strain (at the apex of the dome)	t	actual thickness of the sheet
d_{die}	diameter of the die (inner)		

Figure 1 — Principle of the bulge test

The coordinate origin shall be in the centre of the blank holder. The XY-plane should be parallel to the surface of the blank holder (parallel to the clamped metal sheet before forming). Herein, the x-direction corresponds to the rolling direction. The z-direction shall be normal to the clamped metal sheet before forming, with the positive direction towards the optical sensor.

6 Test equipment

6.1 The bulge test shall be carried out on a machine equipped with a die, a blank holder and a fluid chamber. The proposed equipment is illustrated in Figure 2.

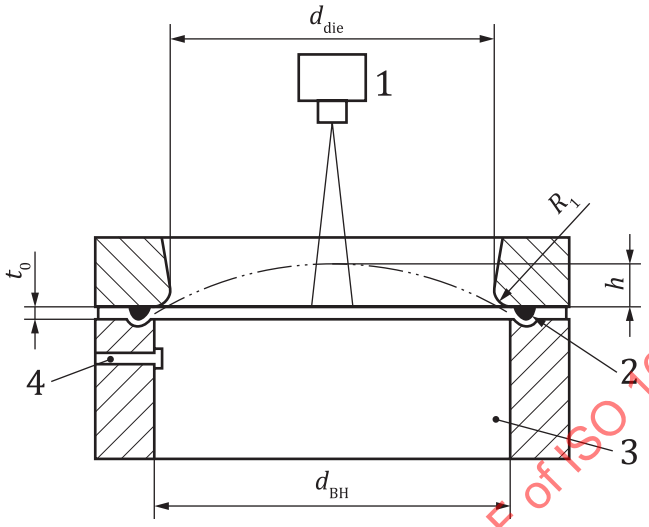

Key

1 deformation measurement system
2 lock bead
3 chamber with fluid
4 pressure measurement system

Figure 2 — Proposal of a testing equipment (principle drawing)

6.2 The layout of the test equipment shall be such that it is possible to continuously measure the outside surface of the test piece continuously during the test, i.e. to be able to determine the deformation of the geometry by recording the evolution of X, Y, Z coordinates of a grid of points on the bulging blank surface, in order to calculate the shape and the true strains in the central area of interest until failure occurs.

6.3 During the test, the system shall be able to measure optically (without contact) the X, Y, Z coordinates of a grid of points on the bulging surface of the specimen. Out of these coordinates, the true strains ε_1 and ε_2 for each point of the selected area, the thickness strain ε_3 and the curvature radius ρ for the apex of the dome are calculated.

6.4 The system should be equipped with a chamber fluid pressure measurement system. An indirect measurement system is also possible. Starting from 20 % of the maximum measured pressure value, the precision should be 1 % of the actual measured value.

6.5 The die, the blank holder and the fluid chamber shall be sufficiently rigid to minimize deformation during testing. The blank-holder force shall be high enough to keep the blank holder closed. Any movement of the test piece between the blank holder and die should be prevented. Typically during the test, the bulge pressure is acting on parts of the blank holder reducing the effective blank-holder force. This shall be taken in consideration when defining the necessary blank-holder force.

6.6 The fluid shall be in contact with the blank surface (without any air bubbles) to prevent energy storage during the test through compressed air bubbles which would lead to higher energy release and greater oil splashing at failure. No fluid shall be lost through the blank holder, die and sheet or elsewhere during the test until failure occurs.

6.7 A lock bead (or comparable geometry in the circular surface), designed to suppress any material flow, is recommended. The lock bead shall not initiate cracks in the material. The lock bead shall be located between blank holder and die. A location close to the die radius is recommended. The lock bead geometry should avoid a curvature and a wrinkling of the blank when closing the tool and prevent the sliding of the blank during the test.

6.8 It is recommended to place glass plates in front of the lenses and the illumination in order to protect the optical measuring system from oil splashing due to blank failure at the end of the test[7],[12]. The plates can be fixed on the blank holder (thick glass) or near the camera lenses and illumination (thinner glass); see Figure 3. The inserted protection shall not disturb the optical measurement quality (see Clause 7). After each test, the glass plates shall be well cleaned without damaging or scratching them and precisely repositioned to not alter calibration. Typically, a calibration of the optical system including the protection increases the measurement quality.

6.9 The smallest die diameter recommended should have a ratio of die diameter to initial thickness $d_{die} / t_0 \geq 33$ (see Figure 2). The radius of the die should not lead to cracks in the blank during the test. A recommendation is $(5 \times t_0)$ to $(15 \times t_0)$ (maximum 15 mm).

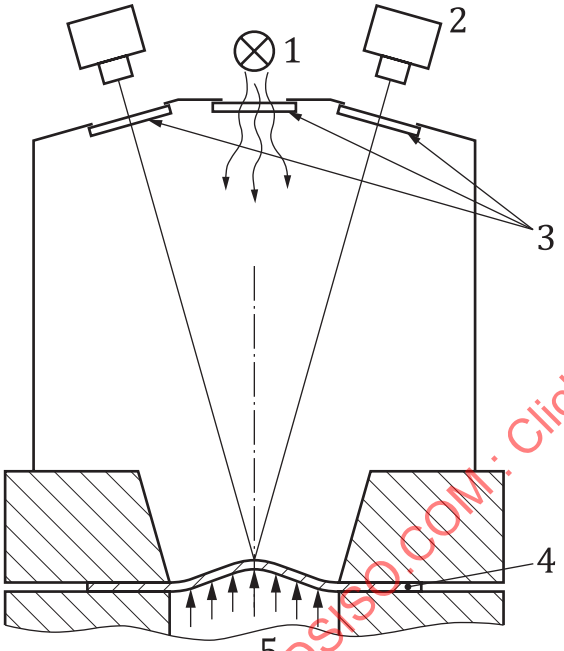

a)

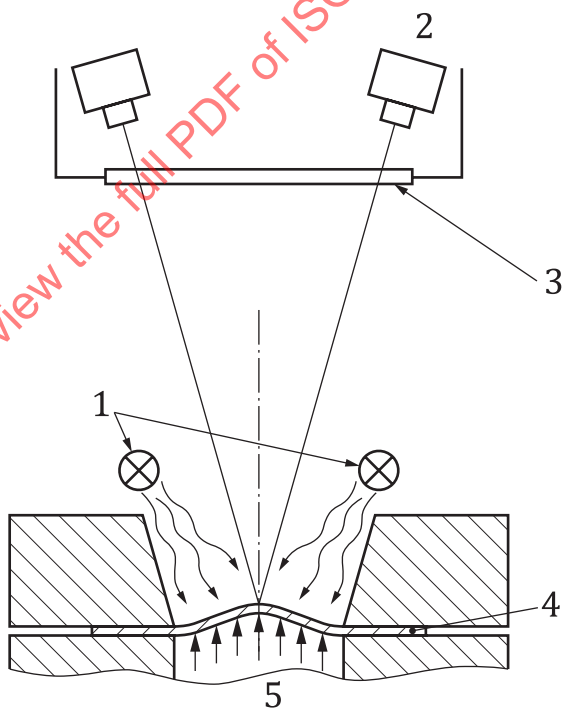

b)

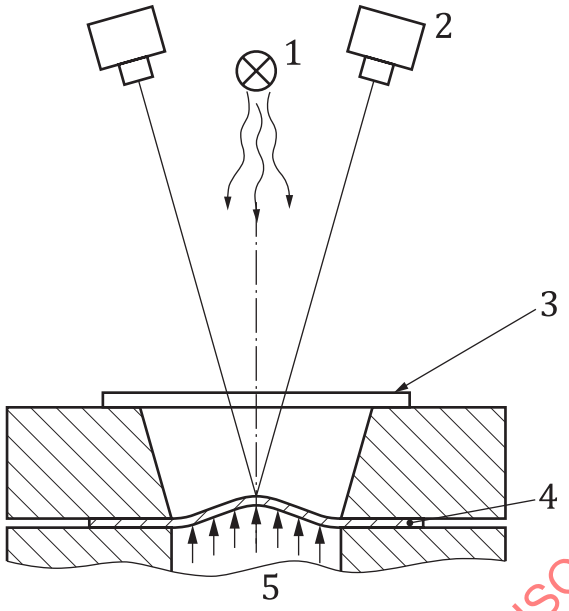

c)

Key

1	lamp	4	test piece
2	cameras	5	fluid
3	glass plates		

Figure 3 — Examples for possible positions of oil shielding plates and lamps

7 Optical measurement system

For the determination of the radius of curvature ρ, and the true strains ε_1 and ε_2, an optical-deformation field measurement system with the following characteristics is recommended.

— Optical sensor based on two or more cameras.

— Measurement area, where $d_{\text{measurement area}} \geq 1/2\ d_{\text{die}}$.

The used measurement area should be larger than a concentric diameter of half the diameter of the blank holder. This area should be observable during the entire forming process for all heights of the drawn blank.

— Local resolution (grid distance between the independent measurement points): The distance $g_{\max}$ between two adjacent points on the unformed blank should follow the requirement:

$$g_{\max} \leq \frac{d_{\text{die}}}{50}$$

— The determination of the curvature requires an accuracy of the z-coordinates in an area with a diameter of $1/2\ d_{\text{die}}$ concentric to the blank holder of

$$rms(dz)_{\text{n}} = \frac{rms(dz) \cdot 100\,\text{mm}}{d_{\text{die}}} \leq 0{,}015\,\text{mm}$$

NOTE The accuracy of the shape measurement can be checked with a test of the optical measurement system (see Annex A).

Accuracy for strain measurement: $rms\ (\varepsilon_1) = 0{,}003$ $rms\ (\varepsilon_2) = 0{,}003$

For each real strain value for the mentioned *rms* (ε) above, the acceptable measurement values are:

$\varepsilon_{real} = 0$ acceptable measurement range: –0,003 … 0,003

$\varepsilon_{real} = 0,5$ acceptable measurement range: 0,497 … 0,503

— Missing measurement points: In order to avoid unbalanced curvature approximations, only the absence of less than 5 % of the measurement points in the concentric area with a diameter = 1/2 d_{die} is acceptable (without interpolation). If adjacent points are missing, the inscribed circle of this area shall not be larger than two points.

8 Test piece

8.1 General

The test piece shall be flat and of such shape that the blank is clamped and material flow is stopped. The use of lock beads is recommended. The edge of the blank shall be outside the lock bead.

The preparation of the blank does not influence the results as long as the surface of the test piece was not damaged (scratches, polishing). The dimension of the outer edges can be circular (preferred) or angular.

8.2 Application of grid

8.2.1 Type of grid

For optical full-field measurement devices, the grid shall fulfil two objectives:

a) the curvature radius determination of the specimens' surface;

b) the strain calculation of the material deformation.

8.2.2 Grid application

Deterministic grids (e.g. squares, circles, dots) should have a strong contrast and have to be applied without any notch effect and/or change in microstructure. Some common application techniques are:

— electrochemical etching, photochemical etching, offset printing and grid transfer;

— stochastic (speckle) patterns which can be applied by spraying paint on the surface of test piece surfaces. Paint adherence to the surface after deformation should be checked. It is possible first to spray a thin, matt white base layer to reduce reflections from the test piece surfaces, then to spray a cloud of randomly distributed black spots (e.g. black spray paint or graphite). The spray shall be both elastic and tough enough not to crack or peel off during deformation. The random distribution of the fine sprayed spots allows the determination of each point of the virtual grid on the specimen. The pattern should have sufficient black/white density and appropriate size features in each point position search area as required by the optical system used.

9 Procedure

9.1 The test shall be carried out at an ambient temperature of (23 ± 5) °C.

9.2 Determine the initial thickness of the test piece to the nearest 0,01 mm.

9.3 Clamp the test piece between blank holder and die. Avoid air bubbles between test piece and fluid to prevent formation of compressed air during testing, leading to stronger oil splashing at failure.

9.4 A constant strain rate of 0,05 s^{-1} is recommended. If a constant strain rate is not possible, a constant forming velocity of the punch or fluid should be guaranteed. In order to avoid big influences in the biaxial stress-strain curve of temperature or strain rate sensitive materials, the bulge test should be conducted in 2 min to 4 min. This time frame guarantees slow and acceptable strain rates and a cost-effective testing time.

The plot of the strain rate versus time is recommended.

9.5 Measure the fluid pressure during the test.

9.6 Measure the X, Y, Z coordinates of the grid on the test piece surface during the test.

9.7 The fluid pressure data and forming data shall be measured and saved at the same time scale. A minimum of 100 values is recommended. In order to represent the whole strain and pressure development, at least 100 images of the bulge testing are recommended.

9.8 The failure of the test piece shall be considered as obtained when a through crack, i.e. a crack which goes through the thickness of the test piece, has occurred. The failure is detected by decreasing fluid pressure, which defines the end of the test.

9.9 A sufficient number of test pieces should be prepared in order to achieve at least three valid tests.

10 Evaluation methods for the determination of the curvature and strains at the pole

For the following explanation of the calculation of the curvature and strains, a spherically shaped surface near the pole is assumed (best-fit sphere). On the last image before failure, as defined in 9.8, the area of the dome with the highest deformation is selected and defined as the position where to determine the true stress and the true thickness strain ε_3. To obtain a stable radius of curvature of the dome, a best-fit sphere can be calculated based on a selected area of points. For this selection, a radius r_1 is defined around the apex of the dome in the last image before bursting and the fit is performed for all forming stages with the same selection of points (Figure 4).

A certain number of the first forming stages (images) are rejected, since the specimen is still too flat for a reliable determination of the best-fit sphere, since the bending radius is very high and the fit is not stable. For robust values of the true strain and thinning in the apex, the average value of a number of selected points is taken. Therefore, a second area is defined by a radius r_2 in a similar manner (see Figure 4).

Based on this procedure, for every forming stage (image) the radius of curvature, the average thickness strains, as well as the corresponding thickness and stress values at the dome apex are calculated. This evaluation can be carried out for different r_1 and r_2 values (see Figure 4).

For a good convergence and robust values, the recommended range of r_1 and r_2 is defined:

$$r_1 = (0{,}125 \pm 0{,}025) \times d_{\text{die}} \tag{1}$$

$$r_2 = (0{,}05 \pm 0{,}01) \times d_{\text{die}} \tag{2}$$

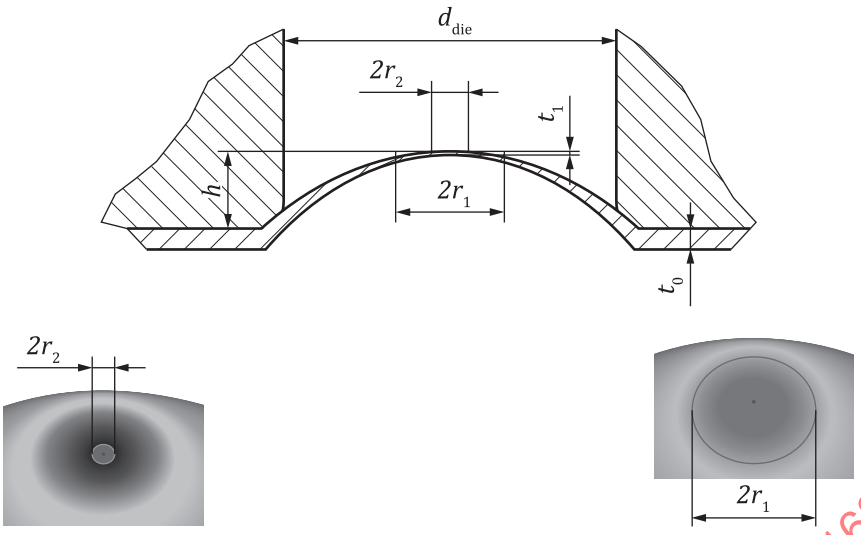

Figure 4 — Choice of r_1 and r_2 for calculation of true stress and true strain for each forming stage

An alternative proposal for the calculation of the curvature and strains is given in Annex B.

11 Calculation of biaxial stress-strain curves

For the calculation of the biaxial stress-strain curves, a simple membrane stress state of a thin-walled spherical pressure vessel is assumed at the centre of the blank. This implies the following simplifications:

a) equi-biaxial stress state:

$$\sigma_1 = \sigma_2 = \sigma_B \tag{3}$$

b) representation of the curvature by the mean curvature radius:

$$\rho = \left[\frac{1}{2}(1/\rho_1 + 1/\rho_2)\right]^{-1} \tag{4}$$

Then the biaxial true stress can be calculated according to the following equation:

$$\sigma_B = \frac{\rho p}{2t} \tag{5}$$

using the fluid pressure p, the curvature radius ρ and the actual thickness t, with

$$t = t_0 \exp(\varepsilon_3) \tag{6}$$

Assuming plastic incompressible deformation of the material and neglecting elastic strains, the total thickness strain for the calculation of the actual thickness can be approximated by the total major and minor true strain:

$$\varepsilon_3 \approx -\varepsilon_1 - \varepsilon_2 \tag{7}$$

Based on the plastic work principle, the biaxial stress-strain curve is a function of the plastic thickness strain: $\sigma_B(-\varepsilon_3^{pl})$, see also Annex C. Assuming an isotropic linear elastic material behaviour and plastic incompressibility, the plastic thickness strain is then given by:

$$\varepsilon_3^{pl} = -\varepsilon_1 - \varepsilon_2 + 2\frac{1-\nu}{E}\sigma_B \tag{8}$$

For the elasticity modulus E and the Poisson ratio ν, literature values are generally sufficient to subtract the elastic contribution, e.g. E = 210 GPa and ν = 0,33 for steel, respectively E = 70 GPa and ν = 0,33 for aluminium alloys.

The ratio of die diameter to thickness should be reasonably high to ensure a near membrane stress state in the test piece, and a negligible influence of bending. For die diameter to thickness ratios lower than 100, it is recommended to check if the bending strains are relatively small compared to the actual thickness strain result ε_3 using the following estimate for the bending strains:

$$\varepsilon_{bending} \approx -\ln\left(1 - \frac{t_0}{2\rho}\exp(\varepsilon_3)\right) \tag{9}$$

NOTE The biaxial stress-strain curve is obtained without any assumption on the type of yield criterion. This biaxial stress-strain curve can be used to identify the equi-biaxial stress point of the yield locus as well as to approximate the material hardening curve beyond uniform elongation.

Annex C gives a proposal for the determination of the equi-biaxial stress point of the yield criterion and for using the biaxial stress-strain curves of hydraulic bulge tests to extrapolate an equivalent stress-strain curve which is based on uniaxial tension tests.

12 Test report

The test report shall contain at least the following information:

a) reference to this document i.e. ISO 16808:2022;

b) identification of laboratory that measured the bulge test values, including the name of operator;

c) identification of material;

d) initial thickness of blank;

e) grid, camera system and software used;

f) position of the protective glasses;

g) geometries of the test equipment;

h) bulge / piston speed;

i) bulge test evaluation method, respectively the parameters for identification of the curvature and the average of strain;

j) number of replications;

k) for each bulge test, a table of values with the history of time, radius ρ, pressure p, absolute value of plastic thickness strain and biaxial true stress;

l) biaxial stress-strain curves of all bulge tests as a plot.

Annex A
(informative)

Test procedure for a quality check of the optical measurement system

A.1 Test procedure

Regarding the recommended quality of the optical measurement system (see Clause 7) and the setup for example according to Figure 3, it shall be taken into account that the additional glass plates in the optical path can have a significant influence. For a check of the final quality for the complete experimental setup, the following procedure (see Figure A.1) is recommended.

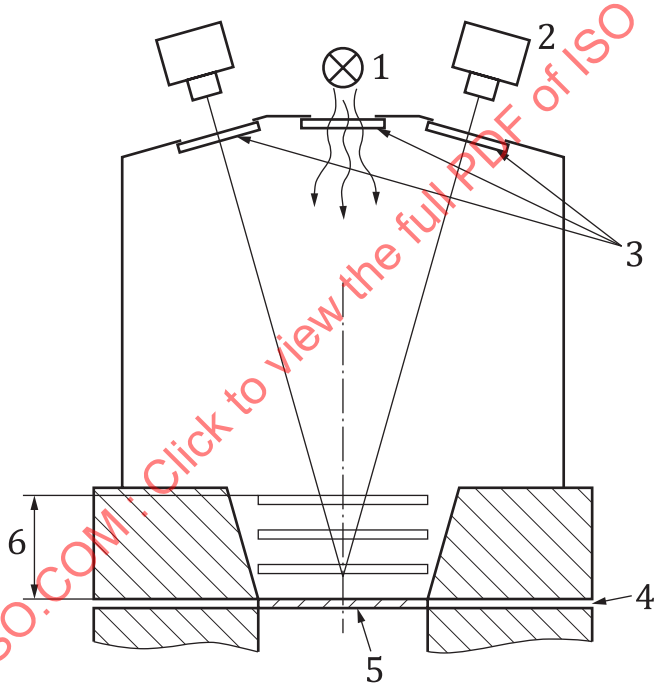

Key

1 lamp
2 cameras
3 glass plates
4 sheet metal
5 reference plate
6 maximum height

Figure A.1 — Quality check of optical measurement system

A rigid test object (e.g. plate, 3-dimensional curved surface) with a diameter ≥ 1/2 d_{die} shall be used. The object shall not to be deformed during the test procedure. The object should have an appropriate surface for the measurement system.

The test object shall be measured on the initial sheet clamping position once without protection glass plates (reference measurement).

The test object shall be measured with the complete measurement setup (including the protection glass plate) in different positions (5 to 10) between initial sheet clamping position and the maximum estimated bulge height h_{max} (see Figure A.1).

A.2 Post-processing

The coordinates for all measurement points in all stages shall be determined.

A rigid body movement correction shall be done by a least square fit, the 3D coordinates from each stage are aligned to the reference measurement. For this fit, a concentric area with a diameter of 1/2 d_{die} shall be used.

The remaining deviations in the *z*-direction (*dz*) describe the loss of quality. An example of a test plate measured in nine different positions is shown in Figures A.2 and A.3.

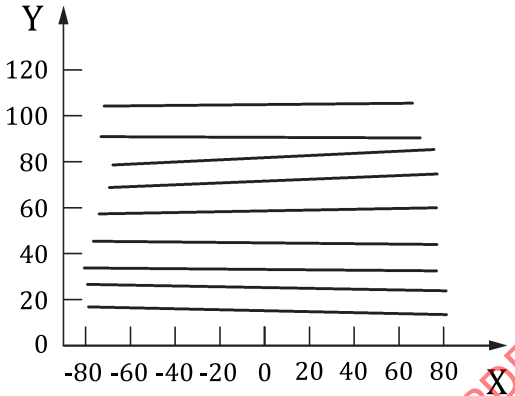

Key

X l_s (in mm)

Y *dz* (in mm)

Figure A.2 — Original displacement *dz* of a cross section of the reference plate (d_{die} = 200 mm)

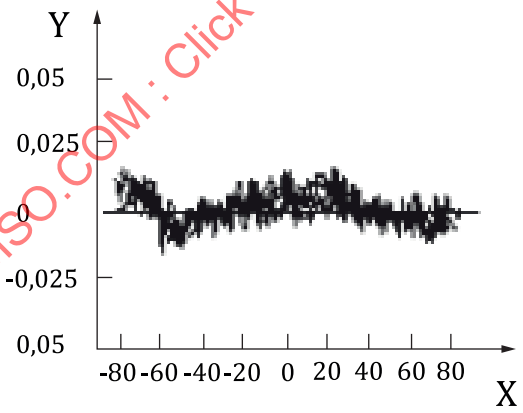

Key

X l_s (in mm)

Y dz_{mv} (in mm)

Figure A.3 — Displacement *dz* of a cross section of the reference plate after movement correction

A.3 Determination of the normalized standard deviation

The standard deviation for *z*, ε_1 and ε_2 (see Clause 7) shall be determined for a concentric area with the diameter of 1/2 d_{die}. In Figure A.4, the determined *rms* (dz_{mv}) is shown based on the given example above.

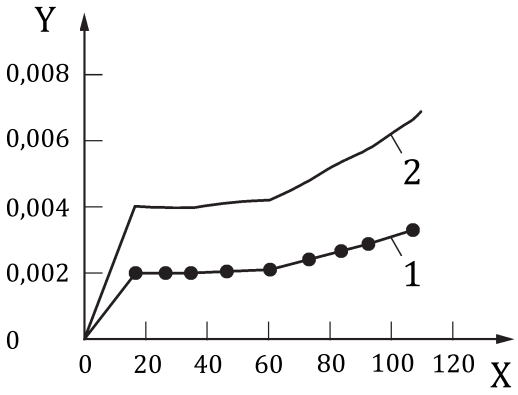

Key

X	*dz* (in mm)	1	original
Y	*rms* (dz_{mv}) (in mm)	2	normalized

Figure A.4 — Original standard deviation *rms* (*dz*) and normalized standard deviation *rms* $(dz_{mv})_n$ after movement correction

For the example in Figure A.4 with a diameter d_{die} = 200 mm, the normalized standard deviation for all positions is smaller than the limit [*rms* $(dz_{mv})_n \leq 0{,}015$ mm].

Annex B
(informative)

Computation of the curvature on the basis of a response surface

B.1 General

The following expression illustrates a response surface based on a full quadratic polynomial function for the determination of the curvature in the dome apex (based on the coordinate system defined in Clause 5). The linear parameters a_i are determined by minimizing the sum of squared residuals. The residuals are defined by the difference between the z-coordinates of the measured shape and corresponding fitted values provided by the response surface.

$$z(x,y)=a_0x^2+a_1y^2+a_2xy+a_3x+a_4y+a_5 \tag{B.1}$$

This procedure is performed for each measured state, selected for the evaluation of the biaxial stress-strain curve. The parameter identification of the response surface is performed on the basis of measurement points, which are inside a sphere (r_1). The point of the measured grid, which exhibits the maximum deformation with respect to the drawing direction, is taken as the midpoint of this sphere and the radius r_1 is given below:

$$r_1=\frac{r_{1\_100}}{100}\cdot d_{\text{die}} \tag{B.2}$$

with

$$r_{1\_100}\leq 10\,\text{mm}$$

The coordinate of the dome apex (x_D, y_D, z_D) is the stationary point of the response surface. The second formula gives the radius with respect to the dome apex ($x = x_D, y = y_D$).

$$\rho=\frac{1}{\kappa} \tag{B.3}$$

$$\kappa=\frac{\kappa_x+\kappa_y}{2}=\frac{\kappa_1+\kappa_2}{2} \tag{B.4}$$

$$\kappa_x=\frac{2a_0}{\left[1+(2a_0x_p+a_2y_p+a_3)^2\right]^{\frac{3}{2}}} \tag{B.5}$$

$$\kappa_y=\frac{2a_1}{\left[1+(2a_1y_p+a_2x_p+a_4)^2\right]^{\frac{3}{2}}} \tag{B.6}$$

B.2 Computation of the material thickness at the dome apex

A sphere (r_2) defines the strain states, which are taken into account for the computation of the material thickness. The midpoint of the sphere is coincident with the dome apex. The radius r_2 is derived from the side length of the measurement grid (SLMG).

$$r_2 = 3 \cdot \mathrm{SLMG} \tag{B.7}$$

The computation of the material thickness is based on the ε_3 field, defined by the coordinates x and y and given at discrete points, depending on the measurement grid. The ε_3 field is determined on the basis of computed ε_1 and ε_2 values under the assumption of the plastic incompressibility and by neglecting the elastic strain contributions. Subsequently, a response surface function is given, which approximates the ε_3 field.

$$\varepsilon_3(x, y) = b_0 x^2 + b_1 y^2 + b_2 xy + b_3 x + b_4 y + b_5 \tag{B.8}$$

The parameters b_i are determined by minimizing the sum of squared residuals. The residuals are defined by the difference between the ε_3 values, obtained from the response surface, and the discrete field resulting from measurement data. The coordinates x_D and y_D are coincident with the dome apex. The following expression gives the relation between the ε_3 strain at the dome apex and the thickness:

$$t = t_0 \cdot e^{\varepsilon_3(x_D, y_D)} \tag{B.9}$$

Annex C
(informative)

Determination of the equi-biaxial stress point of the yield locus and the hardening curve

C.1 General

From the bulge test, equi-biaxial stress-strain curves are obtained where the average of the major and minor stress from the bulge tests is plotted against the absolute value of the plastic true thickness strain. Usually, the true-stress true-strain curve determined from uniaxial tensile test data in rolling direction is used as a reference for material hardening and the calculation of the stress points of the yield locus. By comparing the curves of the stress-strain data of the equi-biaxial stress state with the uniaxial reference curve, the equi-biaxial stress point can be calculated and the equi-biaxial stress-strain curve can be transformed to an equivalent stress-strain curve which provides work hardening data at strains higher than the uniform strain of the tensile test. A procedure for how to determine the equi-biaxial stress ratio and how to scale bulge test results to extend the uniaxial stress-strain curve beyond uniform elongation is described in C.2.

C.2 Procedure

The method described here is one of many procedures for handling the stress-strain data from a bulge test. It is the responsibility of the user to check if the underlying assumptions are sufficiently fulfilled, such that this method is in coherence with the actual material behaviour. If in doubt, it is strongly recommended to consult experts in this field.

In this procedure, the following assumptions are made:

— isotropic hardening;

— the yield locus shape does not change with the strain;

— the work hardening is independent from the strain path (loading path);

— the loading path and strain path of the test is constant;

— the strain rate and temperature of the bulge test is close to the strain rate and temperature of the tensile test. If this condition is not fulfilled, the effect of strain rate and temperature on the material strength should be known, to decide whether a correction is necessary or not.

As a starting point in order to enable extrapolation in the post uniform strain range of the tensile test, the true plastic strain at uniform elongation of the tensile tests, $\varepsilon_{1-\mathrm{UE}}$, in the rolling direction is chosen as a reference value for the equivalent strain, $\varepsilon_{\mathrm{E-ref}}$.

$$\varepsilon_{\mathrm{E-ref}} = \varepsilon_{1-\mathrm{UE}} \tag{C.1}$$

This is considered to be the last valid point of the true stress true strain curve of the tensile test, from where the hardening curve will be extrapolated using bulge test data. Accordingly, the stress at the uniform strain of the tensile tests is used as the reference flow stress, $\sigma_{\mathrm{f-ref}}$, i.e. the ultimate tensile

strength transformed to a true stress. The corresponding reference stress value of the bulge test, $\sigma_{\mathrm{B-ref}}$ are looked up in the following way.

$$\sigma_{\mathrm{B-ref}} \cdot \left|\varepsilon_{3-\mathrm{ref}}\right| = \sigma_{\mathrm{f-ref}} \cdot \varepsilon_{\mathrm{E-ref}} \tag{C.2}$$

In Formula (C.2), $\varepsilon_{3-\mathrm{ref}}$ is defined as the corresponding reference thickness strain for the bulge test.

In the last part of this annex, the theoretical background of this method is explained. Since the bulge test curve is given by discrete values, there will not be a pair of stress and strain which perfectly satisfies condition shown in Formula (C.2). Therefore, the point *m* in the bulge test data matches the following condition:

$$\sigma_{\mathrm{B},m} \cdot \left|\varepsilon_{3,m}\right| \leq \sigma_{\mathrm{f-ref}} \cdot \varepsilon_{\mathrm{E-ref}} \tag{C.3}$$

and

$$\sigma_{\mathrm{B},m+1} \cdot \left|\varepsilon_{3,m+1}\right| \geq \sigma_{\mathrm{f-ref}} \cdot \varepsilon_{\mathrm{E-ref}} \tag{C.4}$$

The requested reference stress of the bulge test can now be computed by simple linear interpolation:

$$\sigma_{\mathrm{B-ref}} = \sigma_{\mathrm{B,m}} + \frac{\sigma_{\mathrm{B},m+1} - \sigma_{\mathrm{B},m}}{\sigma_{\mathrm{B},m+1} \cdot \left|\varepsilon_{3,m+1}\right| - \sigma_{\mathrm{B},m} \cdot \left|\varepsilon_{3,m}\right|} \cdot \left(\sigma_{\mathrm{f-ref}} \cdot \varepsilon_{\mathrm{E-ref}} - \sigma_{\mathrm{B},m} \cdot \left|\varepsilon_{3,m}\right|\right) \tag{C.5}$$

The value of the biaxial stress ratio is obtained by

$$f_{\mathrm{bi}} = \frac{\sigma_{\mathrm{B-ref}}}{\sigma_{\mathrm{f-ref}}} \tag{C.6}$$

With the biaxial stress factor defined in Formula (C.6), the bulge test curve can be transformed into an equivalent strain-stress curve. In combination with uniaxial stress-strain curves from tensile tests, this transformed curve can be used to generate a hardening curve with data extrapolated beyond strain at uniform elongation.

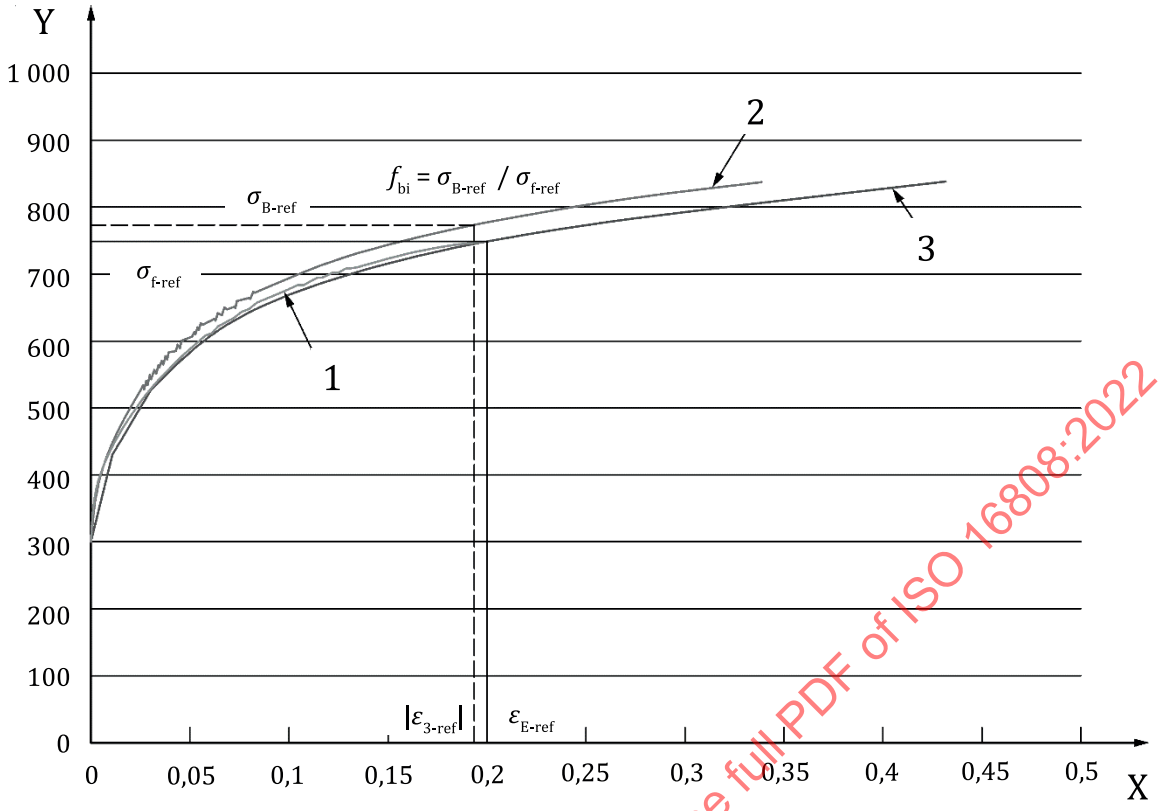

Key

X ε_E, $|\varepsilon_3|$

Y σ_f (in MPa), σ_B (in MPa)

1 σ_f from the uniaxial test

2 σ_B from the bulge test

3 σ_f from the bulge test

Figure C.1 — Example of the uniaxial stress strain and the equi-biaxial stress-strain curve of a material including the biaxial stress calculation of the reference point and the hardening curve based on scaled bulge test results

In Table C.1, it is demonstrated how the equi-biaxial stress factor is calculated and how the uniaxial stress-strain curve is extrapolated by using the bulge test data. Extrapolation is realised by adding the bulge tests data at equivalent strains (given in the columns 9 and 10 in Table C.1) larger than the uniform strain of the tensile test to the uniaxial stress strain curve (given in the columns 2 and 3 in Table C.1). In Table C.2, the example shown in Figure C.1 is represented as a table of numbers according to the procedure of Table C.1.

Table C.1 — Description of the procedure for the calculation of the yield locus parameters and the extrapolation of the hardening curve

Uniaxial curve (RD)				Equi-biaxial curve from the bulge test					
i [a]	$\varepsilon_i = \varepsilon_E$	$\sigma_{f\,i}$	$\sigma_{f\,i} \cdot \varepsilon_i$	k [b]	$\lvert\varepsilon_{3\,k}\rvert$	$\sigma_{B\,k}$	$\sigma_{B\,k} \cdot \lvert\varepsilon_{3\,k}\rvert$	$\varepsilon_{E\,k} = \lvert\varepsilon_{3\,k}\rvert \cdot f_{bi}$	$\sigma_{f\,k} = \sigma_{B\,k} / f_{bi}$
1	$\varepsilon_1 = 0$	$\sigma_{f\,1}$	0	1	$\lvert\varepsilon_{3\,1}\rvert$	$\sigma_{B\,1}$	0	$\varepsilon_{E\,1} = 0$	$\sigma_{f\,1}$
2	ε_2	$\sigma_{f\,2}$	$\sigma_{f\,2} \cdot \varepsilon_2$	2	$\lvert\varepsilon_{3\,2}\rvert$	$\sigma_{B\,2}$	$\sigma_{B\,2} \cdot \lvert\varepsilon_{3\,2}\rvert$	$\varepsilon_{E\,2}$	$\sigma_{f\,2}$
3	ε_3	$\sigma_{f\,3}$	$\sigma_{f\,3} \cdot \varepsilon_3$	3	$\lvert\varepsilon_{3\,3}\rvert$	$\sigma_{B\,3}$	$\sigma_{B\,3} \cdot \lvert\varepsilon_{3\,3}\rvert$	$\varepsilon_{E\,3}$	$\sigma_{f\,3}$
…	…	…	…	…	…	…	…	…	…
…	…	…	…	…	…	…	…	…	…
…	…	…	…	…	…	…	…	…	…
…	…	…	…	…	…	…	…	…	…
…	…	…	…	…	…	…	…	…	…
				m	$\lvert\varepsilon_{3\,m}\rvert$	$\sigma_{B\,m}$	$\sigma_{B\,m} \cdot \lvert\varepsilon_{3\,m}\rvert$	$\varepsilon_{E\,m}$	$\sigma_{f\,m}$
					$\lvert\varepsilon_{3\,m+1}\rvert$	$\sigma_{B\,m+1}$	$\sigma_{B\,m+1} \cdot \lvert\varepsilon_{3\,m+1}\rvert$	$\varepsilon_{E\,m+1}$	$\sigma_{f\,m+1}$
n	$\varepsilon_n = \varepsilon_{E\text{-ref}}$	$\sigma_{f\,n} = \sigma_{f\text{-ref}}$	$\sigma_{f\,n} \cdot \varepsilon_n$	…	…	…	…	…	…
				…	…	…	…	…	…
				…	…	…	…	…	…
				…	…	…	…	…	…

The following quantities in this table are determined as:

n = the last strain point of the uniaxial test being the reference point for the determination of the biaxial stress factor according to Formula (C.5);

M = the last strain point of the bulge test;

m = the point where the following condition is valid for the bulge-test data: $\sigma_{B\,m} \cdot \lvert\varepsilon_{3\,m}\rvert \le \sigma_{f\,n} \cdot \varepsilon_n$ and $\sigma_{B\,m+1} \cdot \lvert\varepsilon_{3\,m+1}\rvert > \sigma_{f\,n} \cdot \varepsilon_n$

The biaxial stress factor is obtained by calculation of a reference biaxial stress point via interpolation of data point m and $m+1$.

$$\sigma_{B-ref} = \sigma_{B_m} + \frac{\sigma_{B_{m+1}} - \sigma_{B_m}}{\sigma_{B_{m+1}} \cdot \lvert\varepsilon_{3_{m+1}}\rvert - \sigma_{B_m} \cdot \lvert\varepsilon_{3_m}\rvert} \cdot \left(\sigma_{f_n} \cdot \varepsilon_n - \sigma_{B_m} \lvert\varepsilon_{3_m}\rvert\right) \quad \text{and} \quad f_{bi} = \frac{\sigma_{B-ref}}{\sigma_{f_n}}$$

[a] i = the index for the points of the uniaxial stress-strain curve determined from the tensile test in rolling direction.

[b] k = the index for the points of the equi-biaxial stress-strain curve determined from the bulge test.

Table C.2 — Example of the procedure for the calculation of the yield locus parameters and the extrapolation of the hardening curve according to Table C.1, graphically represented in Figure C.1

Uniaxial curve (RD)				Equi-biaxial curve from the bulge test					
i [a]	$\varepsilon_i = \varepsilon_{E\,i}$	$\sigma_{f\,i}$	$\sigma_{f\,i} \cdot \varepsilon_i$	k [b]	$\lvert\varepsilon_{3\,k}\rvert$	$\sigma_{B\,k}$	$\sigma_{B\,k} \cdot \lvert\varepsilon_{3\,k}\rvert$	$\varepsilon_{E\,k} = \lvert\varepsilon_{3\,k}\rvert \cdot f_{bi}$	$\sigma_{f\,k} = \sigma_{B\,k} / f_{bi}$
1	0,000	351,7	0,0	1	0,000	306,7	0,0	0,000	297,4
2	0,010	437,1	4,4	2	0,010	441,0	4,4	0,010	427,6
3	0,020	488,7	9,8	3	0,020	502,9	1,1	0,021	487,5
4	0,030	529,0	1,9	4	0,030	546,4	1,4	0,031	529,7
5	0,040	561,9	2,5	5	0,040	579,8	23,2	0,041	562,1
6	0,050	589,4	2,5	6	0,050	607,3	30,4	0,052	588,7
7	0,060	612,7	3,8	7	0,060	629,8	37,8	0,062	610,6
8	0,070	632,6	44,3	8	0,070	649,2	45,4	0,072	629,4
9	0,080	649,8	52,0	9	0,080	666,2	53,3	0,083	645,8
10	0,090	664,8	59,8	10	0,090	681,0	61,3	0,093	660,2
11	0,100	677,8	67,8	11	0,100	694,3	69,4	0,103	673,1
12	0,110	689,2	75,8	12	0,110	706,1	77,7	0,113	684,6
13	0,120	699,2	83,9	13	0,120	717,0	86,0	0,124	695,1
14	0,130	708,1	92,1	14	0,130	726,8	94,5	0,134	704,6
15	0,140	716,1	100,2	15	0,140	735,8	10,0	0,144	713,3
16	0,150	723,1	108,5	16	0,150	744,0	11,6	0,155	721,3
17	0,160	729,5	116,7	17	0,160	751,6	12,3	0,165	728,6
18	0,170	735,2	125,0	18	0,170	758,5	128,9	0,175	735,4
19	0,180	740,4	133,3	19	0,180	764,9	137,7	0,186	741,5
20	0,190	745,2	141,6	20	0,190	770,9	146,5	0,196	747,4
21	0,200	749,5	149,9	21	0,200	776,6	155,3	0,206	752,9
				22	0,210	782,1	164,3	0,217	758,3
				23	0,220	787,4	173,2	0,227	763,4
				24	0,230	792,5	182,3	0,237	768,3
				25	0,240	797,4	191,4	0,248	773,1
				26	0,250	802,3	200,6	0,258	777,8
				27	0,260	806,9	209,8	0,268	782,2
				28	0,270	811,3	219,1	0,279	786,5
				29	0,280	815,7	228,4	0,289	790,8

The following quantities in this table are determined according to the procedure described in Table C.1:

n = 21, the last strain point of the uniaxial test;

M = 42, the last strain point of the bulge test;

m = 20, the point where the following condition is valid for the bulge-test data: $\sigma_{bi\,m} \cdot \varepsilon_{bi\,m} \leq \sigma_{f\,n} \cdot \varepsilon_n$ and $\sigma_{bi\,m+1} \cdot \varepsilon_{bi\,m+1} > \sigma_{f\,n} \cdot \varepsilon_n$.

The biaxial stress factor is obtained by calculation of a reference biaxial stress point via interpolation of data point m and m+1.

$$\sigma_{B-ref} = \sigma_{B_m} + \frac{\sigma_{B_{m+1}} - \sigma_{B_m}}{\sigma_{B_{m+1}} \cdot \lvert\varepsilon_{3_{m+1}}\rvert - \sigma_{B_m} \cdot \lvert\varepsilon_{3_m}\rvert} \cdot \left(\sigma_{f_n} \cdot \varepsilon_n - \sigma_{B_m} \cdot \lvert\varepsilon_{3_m}\rvert\right) = 773{,}1 \text{ and } f_{bi} = \frac{\sigma_{B-ref}}{\sigma_{f_n}} = 1{,}032$$

[a] i = index for the points of the uniaxial stress-strain curve

[b] k = index for the points of the equi-biaxial stress-strain curve